NUMERICAL ANALYSIS OF GRAY GAS RADIATION EFFECTS ON HEAT AND MASS TRANSFER IN AN ANNULAR CAVITY

by

Abdelaziz BOUSSANDEL [a], ***Siham LAOUAR-MEFTAH*** [b*], ***and Noureddine RETIEL*** [a]

[a] Numerical and Experimental Modelling of the Mechanical Phenomena Laboratory, Faculty of Sciences and Technology, Abdelhamid Ibn Badis University, Mostaganem, Algeria
[b] Faculty of Hydrocarbons and Chemistry, M'Hamed Bougara University, Boumerdes, Algeria

Original scientific paper
https://doi.org/10.2298/TSCI230128124B

This study deals with a numerical investigation of coupled double diffusive natural-convection with thermal radiation in an annular cavity containing a gray gas mixture. The black vertical cylindrical walls are maintained at different temperatures and concentrations to create cooperating flows. The finite volume method (using the SIMPLER algorithm) is used to solve the governing equations and the discrete ordinate method (with S8 quadrature) to treat the radiative aspect of the problem. A parametric study illustrating the influence of the optical thickness and the ratio of buoyancy forces, on the flow field and heat and mass transfer for Reyleigh number equal to $5 \cdot 10^6$ and aspect ratio equal to 1, is performed. The numerical results show that gas radiation modifies the flow structure and the distribution of temperature and concentration in the cavity. The effect of permutation of boundary conditions, between the vertical walls, on heat and mass transfer is also considered. The thermal radiation reduces the total heat transfer in the annular space regardless of the configuration of the boundary conditions.

Key words: *annulus space, discrete ordinate method, finite volume method, gas radiation, heat and mass transfer*

Introduction

Due to its widespread application in various engineering disciplines (nuclear reactors, electronic component cooling, and combustion chambers), the problem of double diffusive natural-convection in different geometrical configurations has been the subject of numerous experimental [1-4] and numerical [5-13] researches. Most studies carried out in this field mainly focus on rectangular or square cavities in various arrangements and with different boundary conditions. Unlike the case of Cartesian configurations (rectangular or square), the curvature of the annular geometries modifies the structure of the flows, the distributions of temperature and concentration, as well as the transfers of heat and mass [7, 8]. This behavior is due to the asymmetry of the heat and mass transport phenomena, between the inner and outer surfaces of the annular configurations. Dawood *et al.* [14], Ahmed and Ahmed [15], and very recently Husain *et al.* [16] have carried out an exhaustive review of studies on natural, forced, and mixed convection in horizontal or vertical annulus geometries. Among the considered parameters having important effects on the convection heat transfer, one can site: position of the inner cylinder,

* Corresponding author, e-mail: s.laouar@univ-boumerdes.dz

moving one of the cylinders of the annulus, effect of the size of the annulus, using of porous media or nanofluids, boiling and refrigeration, effect of an external magnetic field, *etc.*

According to these papers, few investigations focused on the coupling of radiative and convective heat transfer are conducted in this area, despite the fact that in several practical situations, the contribution of surface or volumetric radiative transfer must be considered. This last situation occurs when the medium is semi-transparent (contains absorbing species such as water vapour, CO_2, CO, *etc.*) what creates an internal heat source in the medium (result of the difference between the energy absorbed and emitted by each volume element). Among the first studies relative to the problem of heat convection coupled with thermal radiation in an annular space, we mention that of Nichols [17] who examines analytically and experimentally the influence of volumetric radiation on the temperature profile and heat transfer in a turbulent, non-gray gas stream with variable density and temperature-dependent absorption coefficients. The analytical results agree well with those of the experiments carried out by [17]. Moreover, the fact that the absorption of radiation increases the temperature slightly (7%) is also in good agreement with the results of Viskanta's analysis [18]. Onyegegbu [19], who studied analytically the heat transfer in an absorbing and emitting non-gray Boussinesq fluid within the annular gap of two infinitely long horizontal concentric cylinders, concludes that increasing optical thickness enhances total heat transfer and reduces the induced buoyant flow intensity and velocities, and that decreasing boundary emissivity produces the opposite effect. The same problem was later treated by Tan and Howell [20], who conclude that thermal radiation homogenizes the flow structure at high Rayleigh numbers. Weng and Chu [21] studied numerically a similar phenomena but inside a vertical annular cavity. The authors showed that, for different radius ratios and aspect ratios, radiative transfer greatly influences the flow field and temperature distribution inside the enclosure.

In the 2000's, Inaba *et al.* [22] carried out experiments and numerical analyses on surface thermal radiation coupled with natural-convection between two vertical concentric cylinders, for a Rayleigh number ranging from $2 \cdot 10^7$ to $3.5 \cdot 10^9$. The authors have established a Nusselt number correlation as a function of the radius ratio, Rayleigh number, and the temperatures and emissivities of the vertical walls of the cylinders. A similar phenomenon was considered by Shaija and Narasimham [23] but in a horizontal cylindrical annulus. The results for the Grashof number ranging from 10^7 to 10^{10} and surface emissivities varying from 0-0.8 show that surface radiation reduces the convective heat transfer in the annulus and enhances the total Nusselt number. Very recently, Jarray *et al.* [24] reported a numerical analysis of non-gray gas radiation coupled to natural-convection within a cylindrical annulus. The radiative part of the problem was treated by the Ray Tracing method associated to the Statistical Narrow Band correlated-k model. They conclude that radiation has a significant impact on the temperature distribution and structure of the fluid-flow, as well as on heat exchanges in the annulus.

Despite its scientific and technological importance, coupled radiation with double diffusive natural-convection has received far less attention in the cylindrical configuration. The majority of works have been focused on square or rectangular cavities filled with a gray [25, 26] or a non-gray gas [27-31], when temperature and concentration gradients are cooperating or opposing. All results showed that volumetric radiation modifies heat transfer and the characteristics of temperature and concentration fields.

In this study, we analyze numerically the effect of radiative transfer on steady-state double diffusive natural-convection in an annular cavity filled with a gray gas (which emits and absorbs radiation). The enclosure is submitted to cooperating horizontal temperature and concentration gradients (acting in the same direction). A parametric study is performed for an

optical thickness, τ_0, varying from 0-5 and a mass-to-thermal buoyancy ratio $N = 0.8$, 3, and 5. We also analyses the radiative effects on fluid-flow and heat transfer characteristics when the (thermal and mass) boundary conditions are permuted between the inner and outer surfaces of the annulus space.

Mathematical model and numerical method

Physical model

The considered physical system, fig. 1, is a vertical annular domain of height, H, inner radius, r_i, and outer radius r_o. The horizontal walls are impermeable to heat and mass transfer and perfectly reflective, while the vertical walls are black and maintained at different concentrations ($C_L < C_H$) and temperatures ($T_H > T_C$), respectively.

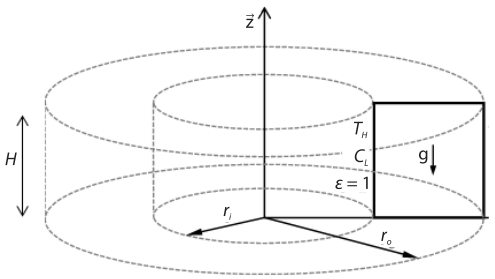

Figure 1. Physical model

Mathematical model

The flow in the cavity is steady, bi-dimensional and laminar. The fluid is Newtonian and incompressible. It absorbs, emits and does not scatter the thermal radiation. All the thermo-physical properties are assumed constant except the density, which varies within the frame of the Boussinesq approximation:

$$\rho = \rho_0\left[1-\beta_T\left(T-T_0\right)-\beta_C\left(C-C_0\right)\right] \tag{1}$$

where

$$\beta_T = -\frac{1}{\rho}\left(\frac{\partial\rho}{\partial T}\right)_{P,C},\ \beta_C = -\frac{1}{\rho}\left(\frac{\partial\rho}{\partial C}\right)_{P,T},\ T_0 = \frac{\left(T_H - T_C\right)}{2} \text{ and } C_0 = \frac{\left(C_H - C_L\right)}{2}$$

The dimensionless governing equations of the double-diffusive natural-convection with radiation in cylindrical co-ordinates can be expressed:

$$\frac{1}{R}\frac{\partial RU}{\partial R}+\frac{\partial W}{\partial Z}=0 \tag{2}$$

$$\frac{\partial U}{\partial\delta}+U\frac{\partial U}{\partial R}+W\frac{\partial U}{\partial Z}=-\frac{\partial P}{\partial R}+\frac{\mathrm{Pr}}{\sqrt{\mathrm{Ra}}}\left(\nabla^2 U-\frac{U}{R^2}\right) \tag{3}$$

$$\frac{\partial W}{\partial\delta}+U\frac{\partial W}{\partial R}+W\frac{\partial W}{\partial Z}=-\frac{\partial P}{\partial Z}+\frac{\mathrm{Pr}}{\sqrt{\mathrm{Ra}}}\nabla^2 W+\mathrm{Pr}\left(\theta+NS\right) \tag{4}$$

$$\frac{\partial\theta}{\partial\delta}+U\frac{\partial\theta}{\partial R}+W\frac{\partial\theta}{\partial Z}=\frac{1}{\sqrt{\mathrm{Ra}}}\nabla^2\theta+\frac{\Theta_0}{\mathrm{Pl}}S_R \tag{5}$$

$$\frac{\partial S}{\partial\delta}+U\frac{\partial S}{\partial R}+W\frac{\partial S}{\partial Z}=\frac{1}{\mathrm{Le}\sqrt{\mathrm{Ra}}}\nabla^2 S \tag{6}$$

where

$$\nabla^2=\frac{1}{R}\frac{\partial}{\partial R}\left(R\frac{\partial}{\partial R}\right)+\frac{\partial^2}{\partial Z^2},\ \mathrm{Ra}=\frac{\mathrm{g}\beta_T\left(T_H-T_C\right)\Delta r^3}{\nu\alpha},\ \mathrm{Le}=\frac{\alpha}{D}$$

$$N = \frac{\beta_C \left(C_{\mathrm{L}} - C_{\mathrm{H}}\right)}{\beta_T \left(T_{\mathrm{H}} - T_{\mathrm{C}}\right)},\ \mathrm{Pl} = \frac{\lambda}{4\Delta r \sigma_B T_0^{\,3}},\ \Delta r = r_{\mathrm{o}} - r_{\mathrm{i}}$$

The dimensionless variables are:

$$R = \frac{r}{\Delta r},\ \ Z = \frac{z}{\Delta r},\ \delta = \frac{\alpha\sqrt{t\mathrm{Ra}}}{\Delta r^2},\ I = \frac{\pi i}{\sigma T_0^{\,4}}$$

$$\theta = \frac{T - T_0}{T_{\mathrm{H}} - T_{\mathrm{C}}},\ \ S = \frac{C - C_0}{C_{\mathrm{H}} - C_{\mathrm{L}}},\ \ P = \frac{p\,\Delta r^2}{\rho\alpha\mathrm{Ra}}$$

$$W = \frac{w\Delta r}{\alpha\sqrt{\mathrm{Ra}}},\ U = \frac{u\,\Delta r}{\alpha\sqrt{\mathrm{Ra}}},\ \Theta_0 = \frac{T_0}{T_{\mathrm{H}} - T_{\mathrm{C}}}$$

In energy eq. (5), the dimensionless radiative term source, S_R, is expressed:

$$S_R\left(R,Z\right) = \tau_0\left[\sum_{m=1}^{N_d} w_m I_m\left(R,Z,\varphi\right) - \left(1 + \frac{\theta}{\Theta_0}\right)^4\right] \tag{7}$$

where $\tau_0\,(=\kappa\Delta r)$ is the optical thickness of the medium, w_m – the weighting coefficient of direction m in the quadrature set, and I_m – the local dimensionless radiation intensity in direction m. This quantity is obtained by solving the radiative transfer equation (RTE) (8), along with the radiative boundary conditions 10(a)-11(b), by discrete ordinates method [32]:

$$\mu_m \frac{1}{R}\frac{\partial\left(RI_m\right)}{\partial R} - \frac{1}{R}\frac{\partial\left(\eta_m I_m\right)}{\partial\varphi} + \xi_m \frac{\partial I_m}{\partial Z} + \tau_0 I_m = \frac{\tau_0}{4\pi}\left(1 + \frac{\theta}{\Theta_0}\right)^4 \tag{8}$$

Initial and boundary conditions

Initially, the fluid is motionless, isothermal (at $\theta_0 = 0$) and homogeneous (at $S_0 = 0$). The boundary conditions used to solve the governing equations, when $H = \Delta r = r_{\mathrm{i}}$:

– At inner hot wall

$$R = R_{\mathrm{i}} = 1 \text{ and } 0 \le Z \le 1:\ U = W = 0,\ \theta = 0.5,\ S = -0.5 \tag{9a}$$

– At outer cold wall

$$R = R_{\mathrm{o}} = 2 \text{ and } 0 \le Z \le 1:\ U = W = 0,\ \theta = -0.5,\ S = 0.5 \tag{9b}$$

– At horizontal walls

$$R_{\mathrm{i}} < R < R_{\mathrm{o}} \text{ and } Z = 0 \text{ or } 1:\ U = W = 0,\ \frac{\partial\theta}{\partial Z} = 0,\ \frac{\partial S}{\partial Z} = 0 \tag{9c}$$

Concerning the radiative boundary conditions, as the vertical walls are black ($\varepsilon = 1$), the leaving intensities correspond to the blackbody emission at walls temperatures:

$$I_m\left(R = 1, Z\right) = \frac{1}{4\pi}\left(1 + \frac{\theta}{\Theta_0}\right)^4 \quad \text{for} \quad \mu_m > 0 \tag{10a}$$

$$I_m\left(R = 2, Z\right) = \frac{1}{4\pi}\left(1 + \frac{\theta}{\Theta_0}\right)^4 \quad \text{for} \quad \mu_m < 0 \tag{10b}$$

and at the horizontal walls (perfectly reflecting, $\varepsilon = 0$), the leaving intensities are:

$$I_m(R,0) = \frac{q^{\text{inc}}(R,0)}{\pi} = \frac{1}{\pi}\sum_{\eta_m<0}|\eta_m| w_m I_m(R,0) \quad \text{for} \quad \eta_m > 0 \tag{11a}$$

$$I_m(R,1) = \frac{q^{\text{inc}}(R,1)}{\pi} = \frac{1}{\pi}\sum_{\eta_m>0}|\eta_m| w_m I_m(R,1) \quad \text{for} \quad \eta_m < 0 \tag{11b}$$

Heat and mass transfer

The average Nusselt numbers (total, convective and radiative), along the internal and external cylinders, are expressed:

$$\text{Nu}_\text{T} = \text{Nu}_\text{C} + \text{Nu}_\text{R} \tag{12}$$

with

$$\text{Nu}_\text{C} = \int_0^1 \left|\frac{\partial\theta}{\partial R}\right|_{R=1\text{or}2} \text{d}Z \tag{13}$$

and

– at inner cylinder wall:

$$\text{Nu}_\text{R} = \frac{\Theta_0}{\text{Pl}}\left[\left(1+\frac{\theta}{\Theta_0}\right)_{R=1}^4 - \sum_{\mu_m<0}|\eta_m| w_m I_m(R,Z,\varphi)\right] \quad \text{for} \quad \mu_m > 0 \tag{14a}$$

– at outer cylinder wall:

$$\text{Nu}_\text{R} = \frac{\Theta_0}{\text{Pl}}\left[\left(1+\frac{\theta}{\Theta_0}\right)_{R=2}^4 - \sum_{\mu_m>0}|\eta_m| w_m I_m(R,Z,\varphi)\right] \quad \text{for} \quad \mu_m < 0 \tag{14b}$$

The average Sherwood number along the sidewalls is determined:

$$\text{Sh} = \int_0^1 \left|\frac{\partial S}{\partial R}\right|_{R=1\text{or}2} \text{d}Z \tag{15}$$

Numerical method

The governing eqs. (2)-(6) along with the appropriate initial and boundary conditions 9(a)-9(c) are solved by the finite volume method [33], based on a SIMPLER algorithm. The centered differences and power law schemes are used for first and second order derivatives, respectively. The numerical calculations are performed using a homemade FORTRAN code. All the calculations are performed using a false transient method. We assumed that a stationary solution is reached when the relative variations, in variables (U, W, θ, ad S) between two successive iterations, are less than 10^{-4}.

Results and discussion

Validation of the calculation code

To check the accuracy of our Fortran code, we first considered the case of pure double diffusive natural-convection in an annular cavity. The obtained average Nusselt and Sherwood numbers are successfully validated against those of Chen *et al.* [8]. The maximum relative error recorded does not exceed 4%, tab. 1. Our flow structures, fig. 2, are also in good agreement with those of Shipp *et al.* [7].

Finally, when the double diffusive natural-convection is combined with volumetric gray gas radiation in a square cavity, our results, fig. 3, compare well with those of Mezrhab *et al.* [25].

Table 1. Average convective Nusselt and Sherwood numbers; Ra = 10^6, Pr = 1, Le = 2, and N = 0.8

$H/\Delta r$	r_0/r_i	[8]		Present work	
		Nu_C	Sh	Nu_c	Sh
1.0	1.5	6.60	8.35	6.69	8.72
	2.0	6.84	8.70	6.72	8.74
	3.0	7.01	8.84	6.87	8.85

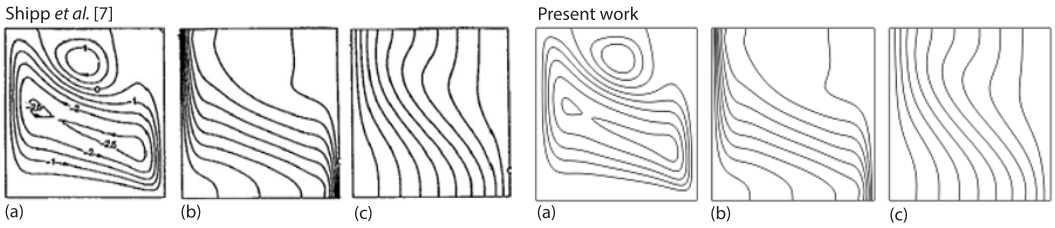

Figure 2. Dimensionless streamlines (a), iso-concentrations (b), and isotherms (c); Ra = 5 · 10^6, Pr = 7, Le = 5, N = –2, $H/\Delta r$ = 1, and r_0/r_i = 2

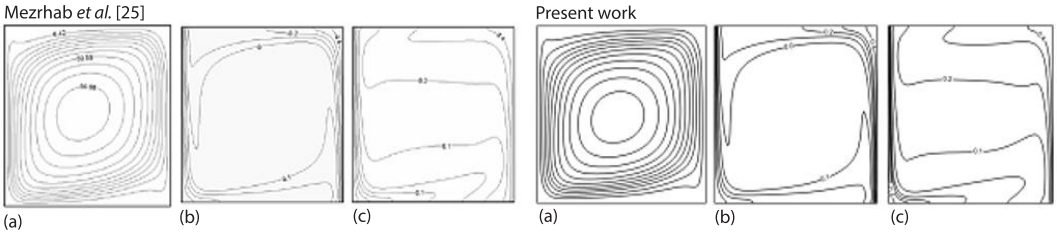

Figure 3. Dimensionless streamlines (a), iso-concentrations (b), and isotherms (c) patterns; Ra = 5 · 10^6, Pr = 0.71, Le = 1, N = 0^+, Pl = 0.02, Θ_0 = 1.5, and τ_0 = 5

Simulation conditions

Our simulations are carried out for the following set of parameters: Ra = 5 ·10^6, Pr = 0.71, Le = 1, $0 < N < 5$, Pl = 0.02, $\Theta_0 = 1.5$, and $0 < \tau_0 < 5$, $H/\Delta r = 1$, and $r_o/r_i = 2$. We also used the S8 quadrature to solve the RTE, and (100×100) non-uniform grid with hyperbolic tangent distribution in R- and Z-directions.

Effect of optical thickness

To estimate the effect of this parameter on the flow structure, and the distribution of temperature and concentration, we consider the case where the thermal buoyancy forces are dominant ($N = 0.8$) and the optical thickness of the medium is varied between $\tau_0 = 0$ (transparent medium) and $\tau_0 = 5$ (optically thick medium). When the fluid is transparen, figs. 4(a_1)-4(c_1), the flow is mono-cellular in the clockwise direction, with a stratified distribution of temperature and concentration in the core region of the cavity (vertical stratification), which justifies the presence of the stagnant fluid in this region. In this case, a cold ($\theta < 0$), and charged fluid in pollutant ($S > 0$) occupies the lower three quarters of the cavity, figs. 4(b_1)-4(c_1), $0 < Z < 0.75$.

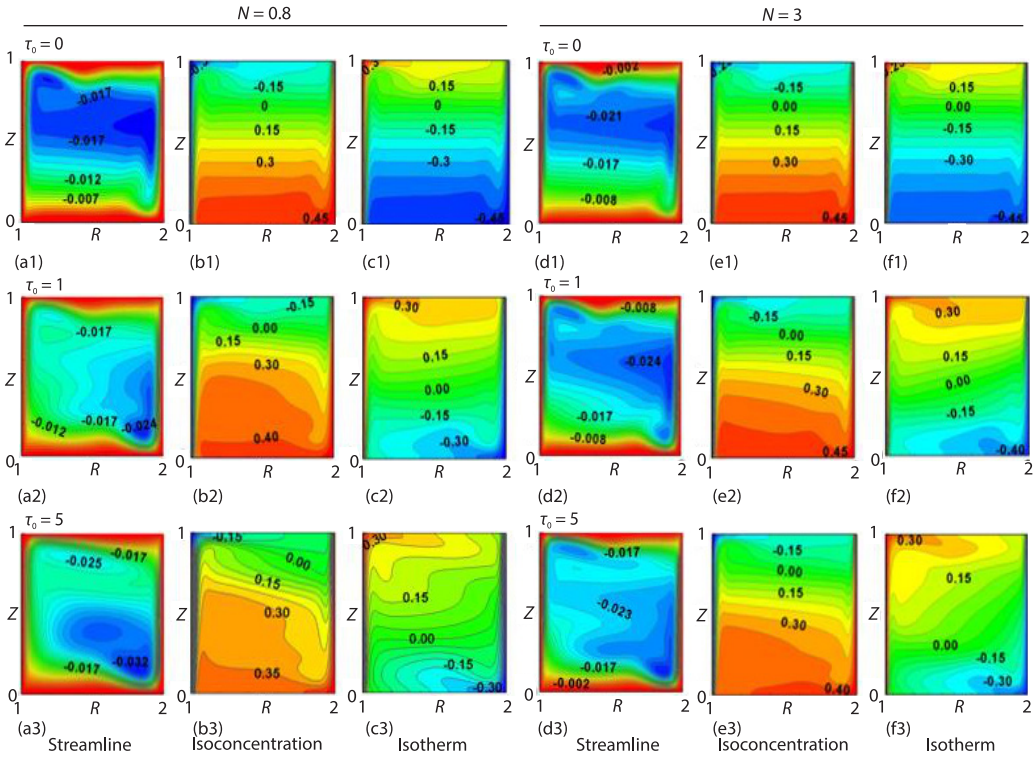

Figure 4. Dimensionless streamline, iso-concentration, and isotherm patterns for different values of buoyancy ratio, *N*, and optical thickness, τ_0

In the presence of gas radiation ($\tau_0 = 1$), figs. 4(a_2)-4(c_2), we notice a modification in the temperature field: the volumetric radiation destroys the vertical stratification of the isotherms, causes their inclinations, fig. 4(c_2), and increases the temperature in the core of the cavity, fig. 5(b). In the vicinity of the horizontal walls, the gradients of temperature (and therefore, the thermal buoyancy forces) are essentially increased near the bottom wall (by absorption of radiation), which causes an acceleration of horizontal and vertical boundary-layers, fig. 6(a), $\tau_0 = 1$. These modifications are accentuated with the increase of fluid opacity, fig. 6(a), $\tau_0 = 5$:

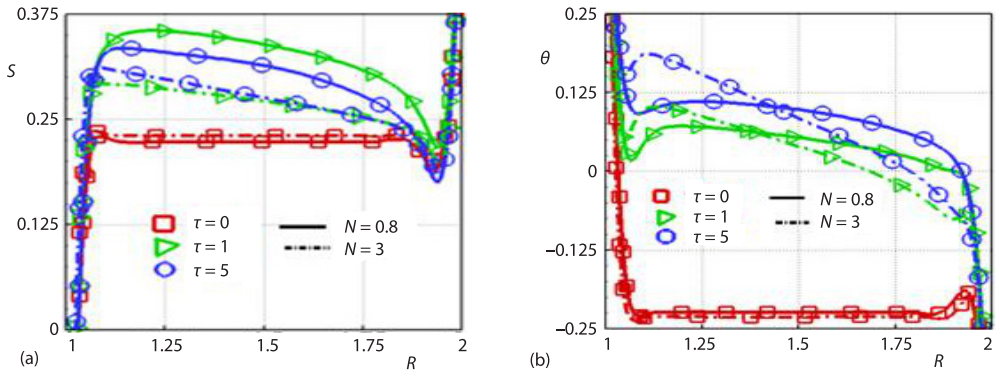

Figure 5 . Dimensionless concentration (a) and temperature (b) profiles at horizontal median plane $Z = 0.5$

the isotherms are distorted, fig. 4(c_3), and the fluid-flow becomes multicellular with a big cell in the lower part of the cavity and a small one in the upper, fig. 4(a_3).

The volumetric radiation also affects the structure of the concentration field, figs. 4(b_2) and 4(b_3): the vertical stratification of the iso-concentration-lines, observed in the transparent gas case, fig. 4(b_1), is inclined in the upper part of the cavity, which indicates the presence of negative gradients of concentration in the *R*-direction, fig. 5(a), $N = 0.8$. In the lower part, the fluid tends to be homogeneous, due to its relatively important acceleration (presence of big cell) compared to the upper region.

Effect of buoyancy ratio N

In this section, the ratio of buoyancy forces, *N*, will be increased from 0.8-3 to study its influence on the flow structures, and heat and mass transfer. The optical thickness, τ_0, of the medium is varied between 0-5.

When increasing *N* (to 3), the mass buoyancy forces become dominant and govern mainly the fluid dynamics. In this situation, the flow structure is less affected by gas radiation: the flow remains (essentially) monocellular in clockwise direction (even at $\tau_0 = 5$), with the appearance of eddy in the upper left part of the cavity, figs. 4(d_2) and 5(d_3). The setting in motion of the cavity core and the acceleration of the boundary-layers are less pronounced than those observed at $N = 0.8$ (dominant thermal forces case), fig. 6(b).

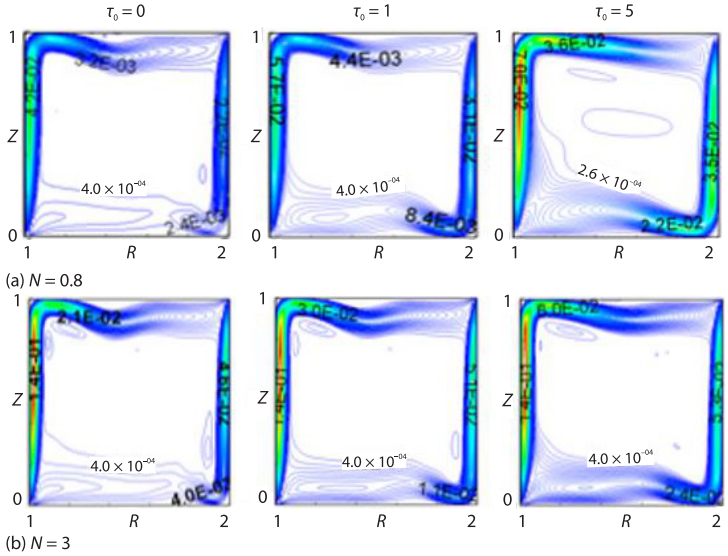

Figure 6. Dimensionless kinetic energy ($0.5[U^2 + W^2]$) for different optical thickness, τ_0: (a) $N = 0.8$ and (b) $N = 3$

The concentration field is also slightly affected by gas radiation, because it is governed by the fluid dynamics less sensitive to thermal radiation: the stratified distribution of iso-concentration-lines, observed with transparent gas, is slightly inclined in the upper part of the cavity. The increase of pollutant concentration, in the cavity core, is weaker than that previously noted at $N = 0.8$, fig. 5(a).

Unlike the dynamic and mass fields, when *N* increases, the effects of gas radiation on thermal field remain important : inclination with distortion of the isotherms, increase of temperature gradients in the vicinity of the horizontal walls, fig. 4(f_2) and 4(f_3), and warming of the cavity center, fig. 5(b), $N = 3$.

Permutation of boundary conditions

Here, we investigate the effects of gas radiation on double diffusive natural-convection, when the vertical boundary conditions are permuted (inner cylinder wall cold at (T_C, C_H) and the outer one hot at (T_H, C_L). The buoyancy force ratio is kept constant at $N = 0.8$ (thermal regime) and the optical thickness of the medium, τ_0, varing from 0-5.

When the gas is transparent ($\tau_0 = 0$), the single-cell flow is established in the counter clockwise direction, with stratified temperature and concentration fields, figs. 7(a)-7(c). The fluid in the upper three quarters of the cavity, fig. 7(c), $0.25 < Z < 1$ is hot ($\theta > 0$) and less charged ($S < 0$) with pollutant, fig. 7(b). Contrary to the initial case (non-permuted boundary conditions), under the influence of the radiation, the fluid is now cooled, and not heated, fig. 5(b), by radiation emission, fig. 9(b), which leads to an increase in temperature gradients at the hot (external) wall and their reduction at the internal cold wall. At horizontal walls, the gradients of temperature (horizontal) are essentially increased near the upper wall, fig. 7(f), rather than the lower wall, fig. 4(c_3).

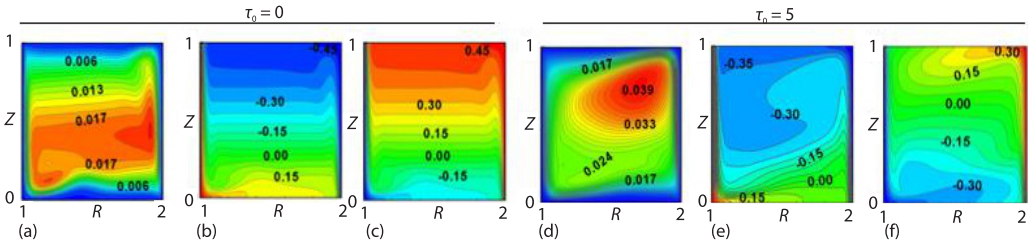

Figure 7. Dimensionless streamlines (a), (d), iso-concentrations (b), (e), and isotherms (c), (f) patterns for $N = 0.8$ and different optical thickness; permuted vertical boundary conditions

Concerning the fluid-flow, fig. 8(b), the core of the cavity is more accelerated (in the upper and not in the lower part of the cavity) than in the previous case, fig. 6(a) and $\tau_0 = 5$. This new fluid dynamics replaces the stratified concentration field by another whose isolines are inclined in the vicinity of the lower wall and practically homogeneous elsewhere, fig. 7(e). Also note that under the influence of radiation, the fluid in the cavity is depleted in absorbing species, fig. 9(a), contrary to the initial case, fig. 5(a).

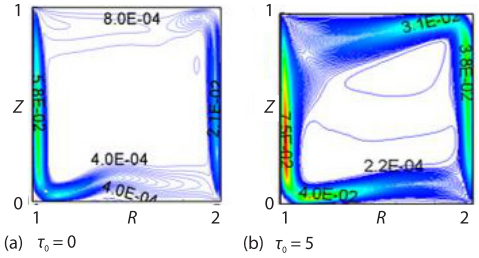

Figure 8. Dimensionless kinetic energy for different optical thickness, τ_0, $N = 0.8$; permuted vertical boundary conditions

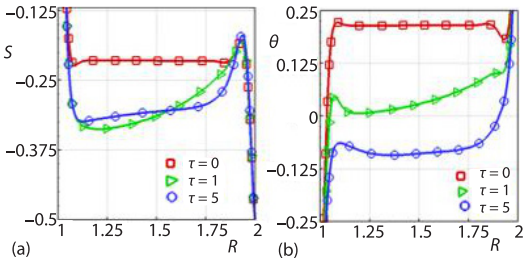

Figure 9. Dimensionless concentration (a) and temperature (b) profiles at median plane $Z = 0.5$, $N = 0.8$; permuted vertical boundary conditions

Heat and mass transfer

Figure 10 displays the average Nu_C and Sherwood numbers, as a function of fluid opacity, τ_0, and buoyancy ratio value, N. We can observe, fig. 10(a) that, regardless of the value

of N (or flow regime), gas radiation reduces the convective flux at the inner hot wall (due to the decrease of temperature gradient) and increases it at the outer cold wall (increase of temperature gradient). We also note a decrease in total heat transfer, Nu_T, tab. 2, due to the attenuation by the fluid of the radiative exchange between the active walls. All of the radiative effects observed on heat transfers intensify as fluid opacity increases, but stabilize beyond τ_0= 3 (approximately).

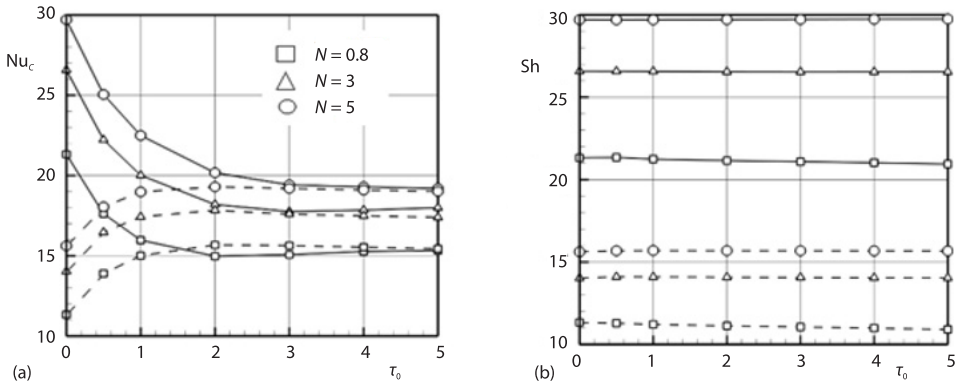

Figure 10. The Nu_C (a) and Sherwood numbers (b) *vs.* τ_0; internal hot wall (solid line) and external cold wall (dashed line)

Concerning the mass transfer, as it is slightly altered by gas radiation, the average Sherwood number, tab. 2(A) and fig. 10(b) is very little affected when the fluid opacity, τ_0, increases, whatever the considered N values.

When the boundary conditions are permuted, the gas radiation reduces the convective flux at the inner cold wall (by weakening the parietal gradient of temperature) and increases it at the outer hot wall (by enhancing the parietal temperature gradient), fig. 11(a). The gas radiation reduces the total heat transfer at the hot wall (outer cylinder) by attenuation of the radiative transfers by the fluid, but in a less remarkable way than in the initial case (*i.e.*, non-permuted boundary conditions), tab. 2(B).

Finally, the mass transfer Sherwood numbers remains less sensitive to gas radiation, as observed previously in non-permuted boundary conditions case, fig. 11(b).

Table 2. The Nu_C, Nu_T, and Sherwood numbers for N = 0.8

τ_0	(A) Hot wall (inner cylinder)			(B) Hot wall (outer cylinder)		
	Nu_C	Nu_T	Sh	Nu_C	Nu_T	Sh
0	21.32	88.77	21.32	11.33	29.77	11.33
1	15.97 (25.1%)	72.92 (17.8%)	21.24 (0.04%)	12.80 (13%)	27.71 (6.9%)	11.24 (0.08%)
5	15.32 (28.1%)	45.59 (48.6%)	20.94 (1.8%)	15.60 (38%)	22.97 (22.8%)	10.98 (3.1%)

Note [%]: relative deviation from the case of a transparent gas (τ_0 = 0).

Conclusions

In this paper, we have studied numerically the influence of gray gas radiation on the laminar double-diffusive natural-convection in an annular cavity, submitted to a cooperating horizontal temperature and concentration gradients, the conclusions are as follows.

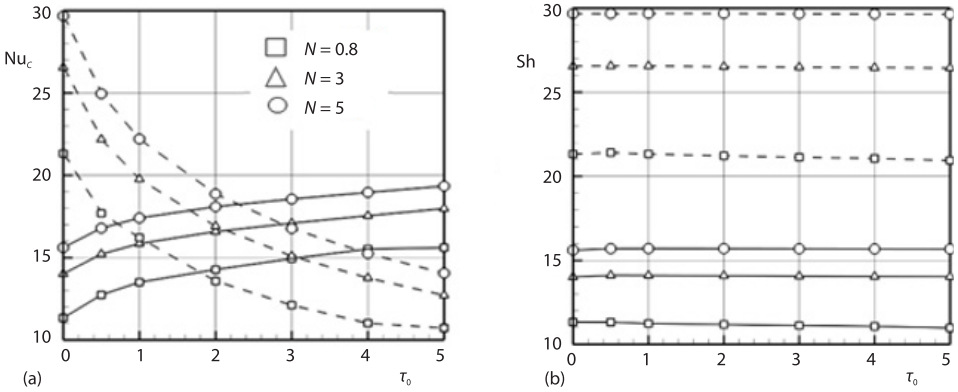

Figure 11. The Nu_C (a) and Sherwood numbers (b) *vs.* τ_0: external hot wall (solid line) and internal cold wall (dashed line); permuted vertical boundary conditions

- When thermal buoyancy forces are dominant (N = 0.8, thermal regime), the stratified distribution of the thermal and mass fields is broken under radiation effects. The core of the cavity is heated, enriched with absorbent species and set in motion (essentially in the lower part), which tends to homogenize the concentration in the lower part of the cavity. These radiative effects intensify with increasing fluid opacity.
- When mass buoyancy forces are dominant (N = 3, mass regime), a similar radiative effects (to those of a thermal regime) are observed, but less pronounced for the dynamic and concentration fields. The effects of gas radiation on the thermal field remain significant.
- Whatever the value of N (or flow regime), gas radiation reduces the convective flux, Nusselt number, (at the internal hot wall and increases it at the external cold wall.The total heat transfer is reduced due to the attenuation by the fluid of the radiative exchange between the active walls, while the mass transfer rate, Sherwood number, is weakly affected.
- When the boundary conditions are permuted, the radiative effects on the local velocities, temperatures and concentrations are totally different from those initially observed before the permutation (the core of the cavity is cooled and depleted in absorbent species, with an acceleration of fluid-flow in the upper part of the enclosure). The convective Nusselt number is reduced at the internal cold wall and increased at the external hot wall, while the Sherwood number remains less sensitive to gas radiation.

Nomenclature

C – concentration, [molm^{-3}]
D – mass diffusivity, [m^{2}s^{-1}]
g – gravitational acceleration, [ms^{-2}]
H – cavity height, [m]
I – dimensionless radiation intensity
i – radiation intensity, [Wm^{-2}sr^{-1}]
Le – Lewis number
N – buoyancy ratio number
Nu – average Nussel tnumber
P – dimensionless pressure
Pr – Prandtl number
Pl – Planck number
p – pressure, [Nm^{-2}]
q^{inc} – incident heat flux at wall, [Wm^{-2}]
Ra – thermal Rayleigh number
r, z – polar co-ordinate, [m]
R, Z – dimensionless polar co-ordinate
S – dimensionless concentration
Sh – Sherwood number
S_R – dimensionless radiative source term
T – local temperature, [K]
t – time, [second]
u, w – orizontal and vertical velocities, [ms^{-1}]
U, W – dimensionless horizontal and vertical velocities
w_m – weight of angular quadrature

Greek symbols

α – thermal diffusivity, [m^2s^{-1}]
β_C – mass expansion coefficient, [m^3mol^{-1}]
β_T – thermal expansion coefficient, [K^{-1}]
δ – dimensionless time
ε – emissivity of the wall
Θ_0 – temperature ratio
θ – dimensionless temperature
κ – absorption coefficient, [m^{-1}]
λ – wave lenght
ν – kinematic viscosity
μ, η, ξ – direction cosines
ρ – density, [kgm^{-3}]
σ – stefan-boltzmann constant, [$Wm^{-2}K^{-4}$]
τ_0 – optical thickness
φ – angular redistribution, [sr]

Subscript

C – cold
H – hot or high
L – low
o,i – outer, inner
m – direction of radiation propagation
0 – reference state

References

[1] Kamotani, Y., *et al*., Experimental Study of Natural-convection in Shallow Enclosures with Horizontal Temperature and Concentration Gradients, *Int. J. Heat Mass Transf.*, *28* (1985), 1, pp. 165-173
[2] Lee, J., *et al*., Natural-Convection in Confined Fluids with Combined Horizontal Temperature and Concentration Gradients, *Int. J. Heat Mass Trans*f., *31* (1988), 10, pp. 1969-1977
[3] Weaver, J. A., Viskanta, R., Natural-Convection in Binary Gases Driven by Combined Horizontal Thermal and Vertical Solutal Gradients, *Exp. Therm. Fluid Sci*., *5* (1992), 1, pp. 57-68
[4] Okorafor, A. A., *et al*., Experimental Investigation of 3-D Flow in a Double-Diffusive Interface System with Lateral Heating, *Exp. Therm. Fluid Sci*., *42* (2012), Oct., pp. 143-153
[5] Trevisan, V., Bejan, A., Combined heat and mass transfer by natural-convection in a vertical enclosure, *Journal Heat Transfer*, *109* (1987), 1, pp. 104-112
[6] Beghein, C., *et al*., Numerical Study of Double-Diffusive Natural-convection in a Square Cavity, *Int. J. Heat Mass Transf*., *35* (1992), 4, pp. 833-846
[7] Shipp, P. W., *et al*., Double-Diffusive Natural-Convection in a Closed Annulus, *Numer. Heat Transf. A*, *24* (1993), 3, pp 339-356
[8] Chen, S., *et al*., Numerical Investigation of Double-Diffusive (Natural) Convection in Vertical Annuluses with Opposing Temperature and Concentration Gradients, *Int. J. Heat Fluid-Flow*, *31* (2010), *2*, pp. 217-226
[9] Koufi, L., *et al*., Numerical Simulation of the CO_2-Diffusion Effect on Low Turbulent Mixed Convection in a Ventilated Room Heated by the Bottom, *Thermal Science*, *23* (2019), 6B, pp. 4783-4796
[10] Ouzaouit, M., *et al*., Numerical Study of the Thermosolutal Convection in a 3-D Cavity Submitted to Cross Gradients of Temperature and Concentration, *Thermal Science*, *25* (2021), 3B, pp. 1923-1933
[11] Moderres, M., *et al.*, Double-Diffusive Natural-convection in a Cavity with an Inner Cylinder Wrapped by a Porous Layer, *Thermal Science*, *26* (2022), 2C, pp. 1841-1853
[12] Kumar, S., *et al*., Applications of Lattice Boltzmann Method for Double-Diffusive Convection in the Cavity: A Review, *Journal Therm. Anal. Calorim*., *147* (2022), May, pp. 10889-10921
[13] Rebhi, R., *et al.*, Non-Darcian Effect on Double-Diffusive Natural-Convection Inside an Inclined Square Dupuit-Darcy Porous Cavity under a Magnetic Field, *Thermal Science*, *25* (2021), 1A, pp. 121-132
[14] Dawood, H. K., *et al*., Forced, Natural and Mixed-Convection Heat Transfer and Fluid-Flow in Annulus: A Review, *Int. Commun. Heat Mass Transf*., *62* (2015), Mar., pp. 45-57
[15] Ahmed, H. E., Ahmed, M. I., Thermal Performance of Annulus with Its Applications; A Review, *Renew. Sust. Energ. Rev*., *71* (2017), May, pp. 170-190
[16] Husain, S., *et al.*, A Review on the Thermal Performance of Natural-Convection in Vertical Annulus and its Applications, *Renew. Sust. Energ. Rev.*, *150* (2021), 111463
[17] Nichols, L. D., Temperature Profile in the Entrance Region of an Annular Passage Considering the Effects of Turbulent Convection and Radiation, *Int. J. Heat Mass Transf*., *8* (1965), 4, pp. 589-607
[18] Viskanta, R., Interaction of Heat Transfer by Conduction, Convection, and Radiation in a Radiating Fluid, *Journal Heat Transfer*, *85* (1963), 4, pp. 318-328
[19] Onyegegbu, S. O, Heat Transfer Inside a Horizontal Cylindrical Annulus in the Presence of Thermal Radiation and Buoyancy, *Int. J. Heat Mass Transf.*, *29* (1986), 5, pp. 659-671
[20] Tan, Z., Howell, J. R., Combined Radiation and Natural-Convection in a Participating Medium between Horizontal Concentric Cylinders, *Proceedings*, Heat Transfer Phenomena in Radiation, Combustion and Fires, Philadelphia, Penn., USA, 1989, pp. 87-94

[21] Weng, L. C., Chu, H. S., Combined Natural-Convection and Radiation in a Vertical Annulus, *Heat Mass Transf.*, *31* (1996), Aug., pp. 371-379
[22] Inaba, Y., *et al*., Natural-Convection Heat Transfer of High Temperature Gas in an Annulus Between Two Vertical Concentric Cylinders, *Heat Transfer-Asian Research*, *34* (2005), 5, pp. 293-308
[23] Shaija, A., Narasimham, G. S. V. L., Effect of Surface Radiation on Conjugate Natural-Convection in a Horizontal Annulus Driven by Inner Heat Generating Solid Cylinder, *Int. J. Heat Mass Transf*., *52* (2009), 25-26, pp. 5759-5769
[24] Jarray, K., *et al*., Effect of Combined Natural-Convection and Non-Gray Gas Radiation on Entropy Generation through a Cylindrical Annulus, *Journal Therm. Anal. Calorim*., *147* (2022), Apr., pp. 4209-4226
[25] Mezrhab, A., *et al*., Numerical Study of Double-Diffusion Convection Coupled to Radiation in a Square Cavity Filled with a Participating Grey Gas, *Journal Phys. D: Appl. Phys*., *41* (2008), 19, pp. 1-16
[26] Moufekkir, F., *et al*., Combined Double-Diffusive Convection and Radiation in a Square Enclosure Filled with Semitransparent Fluid, *Comput. Fluids*, *69* (2012), Oct., pp. 172-178
[27] Meftah, S., *et al*., Coupled Radiation and Double Diffusive Convection in Non-Gray Air-CO_2 and Air-H_2O Mixtures in Cooperating Situations, *Numer. Heat Transf. A*, *56* (2009), pp. 1-19
[28] Ibrahim, A., Lemonnier, D., Numerical Study of Coupled Double-Diffusive Natural-Convection and Radiation in a Square Cavity Filled with a N_2-CO_2 Mixture, *Int. Commun. Heat Mass Transf*., *36* (2009), 3, pp. 197-202
[29] Laouar-Meftah, S., *et al*., Gaz Radiation Effects on Opposing Double-Diffusive Convection in a Non-Gray Air-H_2O Mixture, *Int. J. Therm. Sci.*, *77* (2014), Mar., pp. 38-46
[30] Cherifi, M., *et a*l., Interaction of Radiation with Double-Diffusive Natural-convection in a 3-D Cubic Cavity Filled with a Non-Gray Gas Mixture in Cooperating Cases, *Numer. Heat Transf. A*, *69* (2016), 5, pp. 1-18
[31] Laouar-Meftah, S., *et al*., Impact of Wall Temperature Difference on Heat and Mass Transfers in Gray and Non-Gray Gas Mixtures, *Numer. Heat Transf. A*, *83* (2023), 1, pp. 16-39
[32] Chai, J. C., Patankar, S. V., Discrete-Ordinates and Finite-Volume Methods for Radiative Heat Transfer, in: *Handbook of Numerical Heat Transfer*, 2nd ed., John Wiley and Sons, New Jersey, USA, 2006, pp. 297-323
[33] Patankar, S. V., *Numerical Heat Transfer and Fluid-Flow*, Taylor and Francis, New York, USA, 1980

Paper submitted: January 28, 2023
Paper revised: April 19, 2023
Paper accepted: May 2, 2023